JES
JOURNAL OF ENVIRONMENTAL SCIENCES
ISSN 1001-0742
CN 11-2629/X
December 1, 2014 Volume 26 Number 12
www.jesc.ac.cn

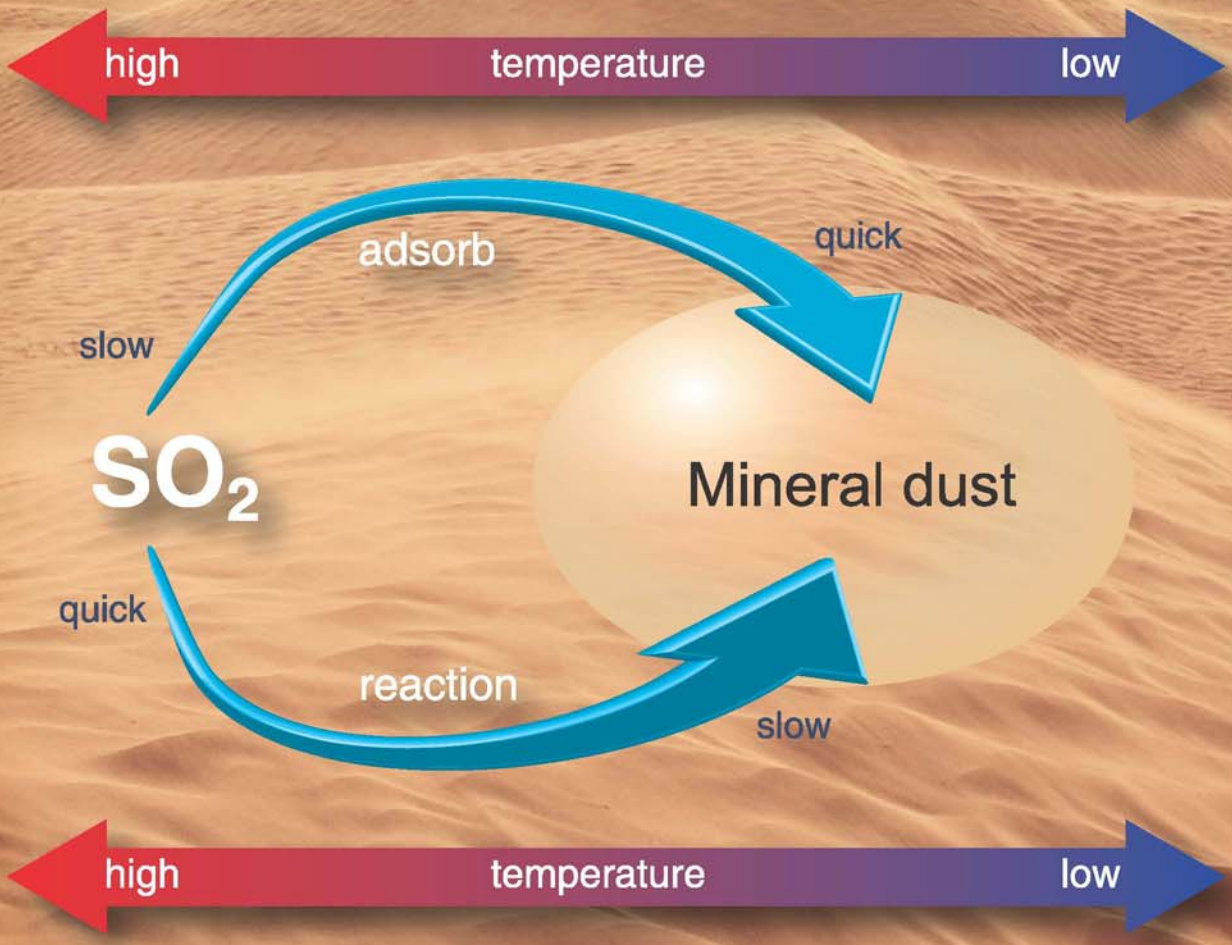

ELSEVIER
Science Press
Sponsored by
Research Center for Eco-Environmental Sciences
Chinese Academy of Sciences

Journal of Environmental Sciences Volume 26 Number 12 2014

www.jesc.ac.cn

CONTENTS

Available online at www.sciencedirect.com

ScienceDirect

www.journals.elsevier.com/journal-of-environmental-sciences

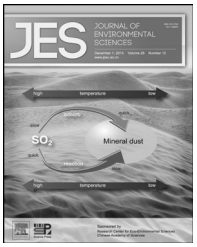

Removal of formaldehyde over $Mn_xCe_{1-x}O_2$ catalysts: Thermal catalytic oxidation *versus* ozone catalytic oxidation

Jia Wei Li[1], *Kuan Lun Pan*[1], *Sheng Jen Yu*[2], *Shaw Yi Yan*[2], *Moo Been Chang*[1,*]

1. *Graduate Institute of Environmental Engineering, National Central University, Chungli 32001, Taiwan, Chinese Taipei*
2. *Industrial Technology Research Institute, Hsinchu 31040, Taiwan, Chinese Taipei*

ARTICLE INFO

Article history:
Received 15 January 2014
Revised 14 April 2014
Accepted 16 May 2014
Available online 22 October 2014

Keywords:
Formaldehyde
Volatile organic compounds
Indoor air pollutant
Thermal catalytic oxidation
Ozone catalytic oxidation

ABSTRACT

$Mn_xCe_{1-x}O_2$ (x: 0.3–0.9) prepared by Pechini method was used as a catalyst for the thermal catalytic oxidation of formaldehyde (HCHO). At x = 0.3 and 0.5, most of the manganese was incorporated in the fluorite structure of CeO_2 to form a solid solution. The catalytic activity was best at x = 0.5, at which the temperature of 100% removal rate is the lowest (270°C). The temperature for 100% removal of HCHO oxidation is reduced by approximately 40°C by loading 5 wt.% CuO_x into $Mn_{0.5}Ce_{0.5}O_2$. With ozone catalytic oxidation, HCHO (61 ppm) in gas stream was completely oxidized by adding 506 ppm O_3 over $Mn_{0.5}Ce_{0.5}O_2$ catalyst with a GHSV (gas hourly space velocity) of 10,000 hr^{-1} at 25°C. The effect of the molar ratio of O_3 to HCHO was also investigated. As O_3/HCHO ratio was increased from 3 to 8, the removal efficiency of HCHO was increased from 83.3% to 100%. With O_3/HCHO ratio of 8, the mineralization efficiency of HCHO to CO_2 was 86.1%. At 25°C, the p-type oxide semiconductor ($Mn_{0.5}Ce_{0.5}O_2$) exhibited an excellent ozone decomposition efficiency of 99.2%, which significantly exceeded that of n-type oxide semiconductors such as TiO_2, which had a low ozone decomposition efficiency (9.81%). At a GHSV of 10,000 hr^{-1}, $[O_3]/[HCHO] = 3$ and temperature of 25°C, a high HCHO removal efficiency (≥81.2%) was maintained throughout the durability test of 80 hr, indicating the long-term stability of the catalyst for HCHO removal.

© 2014 The Research Center for Eco-Environmental Sciences, Chinese Academy of Sciences. Published by Elsevier B.V.

Introduction

Indoor air quality (IAQ) is an issue of great public concern, because lifestyle of people has changed from outdoor to indoor in recent years, typically, people in metropolitan areas spend more than 80% of time in indoor environments. Consequently, governments around the world have strictly regulated indoor air quality to protect human health. Indoor air pollutants are composed of different substances, including volatile organic compounds (VOCs), carbonyl compounds (CO, CO_2), and bio-aerosol and they are emitted from various sources such as burning and cooking, construction materials, the atmospheric environment and others (Shaughnessy et al., 1994; Daisey et al., 2003). Among these indoor air pollutants, formaldehyde (HCHO) is commonly detected in airtight buildings, and it has been recognized as a strong toxicity gas for human body. Sources of HCHO are very wide such as construction materials, paints, cosmetics, cleaning agents, disinfectants, cigarette smoke, and printing ink. For short-term exposure, HCHO may irritate the nose and eyes and it further causes burning sensations in the throat, difficulty in breathing and serious diseases such as respiratory tract and nasal tumors if exposed at a long-term.

Previous studies indicated that various methods including physical adsorption and thermal catalytic oxidation (TCO) can be utilized to reduce HCHO concentration (Imamura et al., 1994; Sekine, 2002; Álvarez-Galván et al., 2004; Tang et al., 2006a; Zhang et al., 2006; Li et al., 2008; Zhang et al., 2009; An et al., 2011; Ma et al., 2011). However, adsorbents are effective for only a short period owing to their limited adsorption capacities, therefore, it may not

* *Corresponding author*. E-mail: mbchang@ncuen.ncu.edu.tw (Moo Been Chang).

http://dx.doi.org/10.1016/j.jes.2014.05.030
1001-0742/© 2014 The Research Center for Eco-Environmental Sciences, Chinese Academy of Sciences. Published by Elsevier B.V.

jesc.ac.cn

be suited for controlling indoor air pollution, while TCO is regarded as one of the most promising approaches for removing HCHO, and it involves oxidizing HCHO to harmless carbon dioxide and water by using an appropriate catalyst. In past studies, noble metal and transition metal oxides are commonly applied as a catalyst for oxidation of HCHO. Noble metal catalysts (Pd, Au or Pt) potentially exhibit high activity at moderate or even room temperatures (Imamura et al., 1994; Álvarez-Galván et al., 2004; Li et al., 2008; Zhang et al., 2009; Ma et al., 2011), but high cost limits their application. Chen et al. (2013) applied Au/CeO_2 as a catalyst for the oxidation of HCHO at room temperature, with GHSV of 143,000 hr^{-1}, RH of 50%, and inlet HCHO concentration of 80 ppm. The results indicate that conversion efficiency of HCHO achieved with Au/CeO_2 reaches 100% (Chen et al., 2013). On the contrary, transition metal oxides (including CuO, Co_3O_4, NiO, Fe_2O_3, and MnO_x) are relatively abundant and inexpensive (Sekine, 2002; Tang et al., 2006b; An et al., 2011; Silva et al., 2004; Zhou et al., 2011). Furthermore, activities of transition metal oxides can be increased by doping other elements, and some investigations have focused on their use in place of costly noble metals (Sekine, 2002; Ma et al., 2011; Zhou et al., 2011; Góra-Marek and Datka, 2008; Gracia et al., 2000; Imamura et al., 1996; Luo et al., 1999). For example, Mn-based catalyst shows good performance for oxidation of HCHO at 75°C as Co is added into Mn (Shi et al., 2012a), in addition, CeO_2 is often used as a good promoter due to high oxygen storage capacity. As CeO_2 is added into MnO_x, the partial substitution of Ce^{4+} with Mn^{4+} in the lattice of CeO_2 improves its oxygen storage capacity, redox properties, thermal resistance, and catalytic activity (Luo et al., 1999). However, most studies indicate that transition metal oxides must operate at high temperature (>200°C) for good performance. Hence, it is not suitable for indoor air quality application. Furthermore, the storage-oxidation process can be also applied for the oxidation of HCHO. The storage-oxidation process implies that HCHO can be first adsorbed on the catalyst surface, and then oxidized into CO_2 and H_2O which are further desorbed by increasing temperature. Shi et al. (2012b) utilized $Ag–MnO_x–CeO_2$ as a catalyst to adsorb and convert HCHO, and the results indicate that this catalyst shows good performance for HCHO removal, but its operating temperature has to be maintained at high than 80°C for complete oxidation of HCHO (Shi et al., 2012b). Reducing the temperature needed for the catalytic reactions is important to save energy and enable their application in IAQ management.

Ozone has been widely used in various environmental applications both in the liquid and gas phases (Oyama, 2000). Previous studies indicate that catalyst oxidation processes in which ozone is utilized to produce oxidants have been investigated and have potential for removing various hazardous compounds especially at low-temperatures (<100°C), including VOCs, CO, cyclohexane, and benzene, and even dioxins can be oxidized by ozone catalytic oxidation process (OZCO) (Gervasini et al., 1996; Einaga and Futamura, 2004a,b, 2005; Konova et al., 2006; Stoyanova et al., 2006; Wang et al., 2011).

OZCO has many unique characteristics, including effectiveness at low temperature and the use of inexpensive p-type transition metal oxides (Dhandapani and Oyama, 1997) as catalysts. Generally, Mn-based is one of the most effective catalysts because it has high activity in ozone decomposition at ambient temperature (Einaga and Futamura, 2004a, 2005; Wang et al., 2011; Dhandapani and Oyama, 1997).

In this work, we attempted to apply TCO and OZCO processes, respectively, to remove HCHO by using Mn-based catalysts. In the TCO process, $Mn_xCe_{1-x}O_2$ catalysts with various Mn/Ce ratios and $Mn_xCe_{1-x}O_2$ mixed oxide with added copper are utilized to decrease reaction temperature and to determine the effect of various supports on the oxidation of HCHO. Then the $Mn_xCe_{1-x}O_2$ of optimum ratio is used to decompose ozone, and further achieve oxidation of HCHO for OZCO process. The effects of O_3/HCHO ratio on HCHO removal are studied. Finally, the effectiveness of OZCO in HCHO removal is compared with that of TCO.

1. Experimental

1.1. Catalyst preparation

$Mn_xCe_{1-x}O_2$ (Mn)/(Mn + Ce) (x: 0.3–0.9, molar ratio) was prepared by the Pechini method. Cerium nitrate ($Ce(NO_3)_3{\cdot}6H_2O$), manganese nitrate tetrahydrate ($Mn(NO_3)_2{\cdot}4H_2O$) and citric acid (citric acid/(Mn + Ce) = 2.0, molar ratio) were dissolved in water to form a 1 mol/L solution, which was gradually heated to 85°C, and maintained for 1 hr with stirring. Then, ethylene glycol was gradually added to the solution at 90°C for 2 hr with stirring, forming a yellowish gel. The gel was dried at 110°C for 12 hr and then calcined at 500°C for 6 hr with air. In addition, the supports with a copper loading of 5 wt.% CuO_x was prepared by the classical incipient impregnation of an aqueous solution of copper nitrate trihydrate ($Cu(NO_3)_2{\cdot}3H_2O$). It was dried overnight at 110°C, and then calcined at 500°C for 6 hr with air.

1.2. Characterization of catalysts

X-ray diffraction (XRD) patterns were recorded using an X-ray diffractometer (D8AXRD Bruker, Germany) with Cu-Kα radiation. The radiation (ë = 1.5415 Å) was generated by an X-ray gun that was operated at 40 kV and 40 mA. Diffraction patterns were obtained within a 2è rang of 10°–70° at a scanning rate of 6°/min.

Brunauer Emmett Teller (BET) surface areas, pore diameter, and pore volume were measured using an ASAP2010 (ASAP2010 Micromeritics, USA). Sample morphology and dispersion were characterized by scanning electron microscopy (S80 JEOL, Japan). An energy dispersive spectroscopic (EDS) analysis yielded the precise elemental composition of materials with a high spatial resolution.

1.3. Catalytic activity measurement

The catalytic activity of the catalysts in the oxidation of HCHO was evaluated in a fixed-bed reactor at atmospheric pressure. The reactor was equipped with a temperature controller, which was used to maintain in the range 25–450°C. The internal diameter of the reactor was 1.3 cm and 300 mg of catalyst (75–100 mesh) was loaded into it. Gaseous HCHO was generated by passing a stream of air through the formalin solution in a thermostatic water bath. A mixture of air with 33 and 61 ppm HCHO, respectively, was introduced into the reactor to serve as reactants. Fig. 1 shows the experimental system used to evaluate the HCHO removal by TCO or OZCO. Ozone was synthesized with pure oxygen supplied by O_2 cylinder using an ozone generator (OZSD-3000A Ebara, Japan). The total flow rate of the feeding gas was 0.6 L/min, yielding a gas hourly space velocity (GHSV) of approximately 10,000 hr^{-1}. The HCHO and O_3 concentrations of exhaust were measured by using a spectrophotometer (GENESYS 10S UV–Vis Thermo Scientific, USA).

Gaseous products of catalytic oxidation were analyzed using a Fourier transform infrared spectrophotometer (Nicolet 6700 Thermo Scientific, USA). Data were collected when the catalytic reaction reached steady-state conditions. The

jesc.ac.cn

efficiencies of HCHO removal, ozone decomposition and mineralization are calculated, respectively, by the following equations:

$$\text{HCHO removal} = \frac{[\text{HCHO}]_{\text{inlet}} - [\text{HCHO}]_{\text{outlet}}}{[\text{HCHO}]_{\text{inlet}}} \times 100\% \quad (1)$$

$$\text{Ozone decomposition}(\%) = \frac{[\text{Ozone}]_{\text{inlet}} - [\text{Ozone}]_{\text{outlet}}}{[\text{Ozone}]_{\text{inlet}}} \times 100\% \quad (2)$$

$$\text{Mineralization efficiency}(\%) = \frac{[CO_2]_{\text{outlet}}}{[\text{HCHO}]_{\text{inlet}}} \times 100\% \quad (3)$$

where, $[\,]_{\text{inlet}}$ and $[\,]_{\text{outlet}}$ are species concentrations measured before and after the reactor, respectively.

2. Results and discussion

2.1. Characterization of the catalysts

Fig. 2 displays the X-ray powder diffraction patterns of the $Mn_xCe_{1-x}O_2$ catalysts. In the XRD patterns of pure MnO_x and CeO_2, the major sharp diffractions at 2θ = 12.7, 18.0, 25.6, 37.4, 41.8 and 49.7° are primarily attributed to MnO_2 (Tang et al., 2006b). For XRD pattern of the pure fluorite-type oxide, the diffraction peaks at 2θ = 28.5, 33.0, 47.4 and 56.4° are attributed to CeO_2 (Tang et al., 2006b). Fig. 2 shows that the samples with Mn fractions (*x*) of less than 0.5 yielded only diffraction peaks associated with the cubic fluorite structure. However, those with Mn fractions (*x*) greater than 0.5 yielded weak diffraction peaks associated with MnO_2 along with broader diffraction peaks from cubic CeO_2. The diffraction pattern of $Mn_xCe_{1-x}O_2$ at Mn/(Mn + Ce) is <0.5, implying that Mn was incorporated into CeO_2 lattice to form a solid solution that maintained the fluorite structure. This result is consistent with a recent report on the structural features of $Mn_xCe_{1-x}O_2$ mixed oxides, which revealed that the crystalline phase depended strongly on the molar proportions of manganese and cerium oxides (Tang et al., 2006b).

Table 1 summarizes BET surface areas of the catalysts. The results indicate that the Cu-loaded catalysts had a smaller surface area because Cu partially blocks pore of supports. The surface areas of $Cu/Mn_xCe_{1-x}O_2$ and $Mn_xCe_{1-x}O_2$ were only 39.2 and 39.3 m^2/g, respectively, because the gel of manganese and cerium hydroxides and the possible interaction during calcination effectively produce crystal growth solid solution of the $Mn_xCe_{1-x}O_2$ mixed oxide. The activities of these catalysts for HCHO oxidation will be discussed in a later section.

2.2. Effect of manganese loading on HCHO removal

In order to determine the effects of the fraction of incorporated manganese on the oxidation of HCHO, modified $Mn_xCe_{1-x}O_2$ was prepared by the Pechini method for testing. As presented in Fig. 3, the HCHO removal efficiency changed with the modified catalysts and temperature. Increasing temperature not only provides more energy and the effective probability of collision, but also excites oxygen deep in the catalyst lattice to the surface of the catalyst, where it is desorbed, then forming oxygen vacancies. Fig. 3 shows that $Mn_xCe_{1-x}O_2$ must be utilized at approximately 300°C to ensure complete HCHO oxidation. The activity of the mixed oxides clearly depended on the amount of Mn present. The relevant curves are frequently characterized by two parameters T_{50} and T_{100}. T_{50} is defined as the temperature required to remove 50% of the pollutant, while T_{100} is the temperature required to achieve 100% removal. The T_{100} values for the removal HCHO of $Mn_xCe_{1-x}O_2$, with x = 0.3, 0.5, 0.7, and 0.9 are 285, 270, 295 and 310°C, respectively. The fractions of Mn in descending order of activity are: x = 0.5 > x = 0.3 > x = 0.7 > x = 0.9. Interestingly, x = 0.5 has the lowest T_{100} of 270°C, this is 40°C lower than that of x = 0.9, at which the highest T_{100} of 310°C is observed. From the above results, incorporating a suitable amount of manganese increases the catalytic

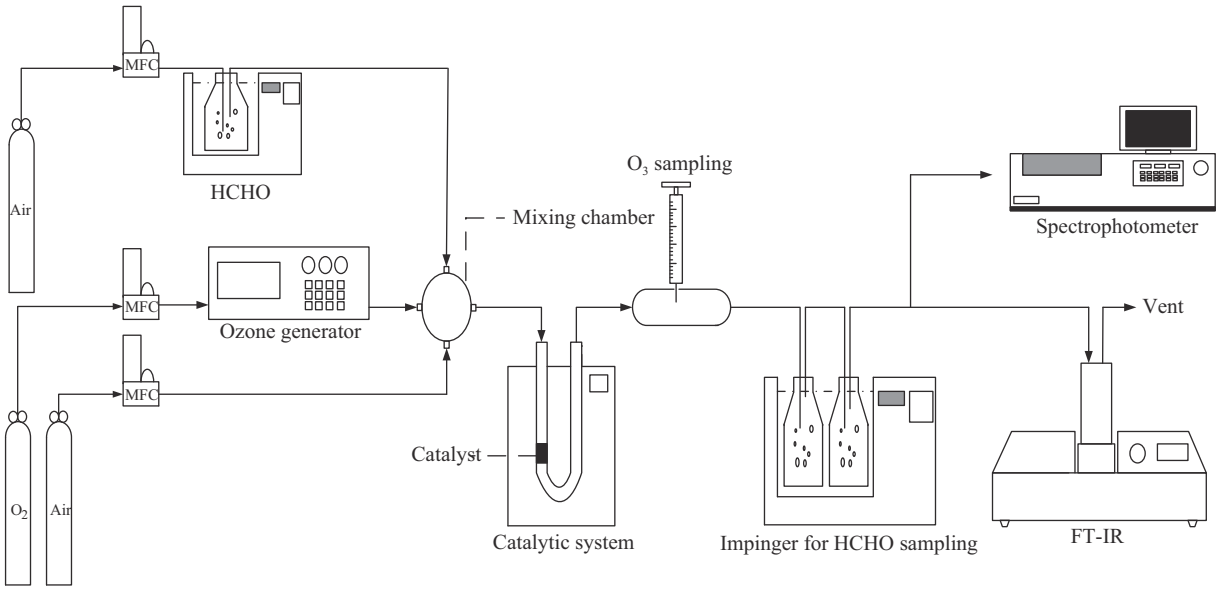

Fig. 1 – Schematic diagram of the experimental setup for formaldehyde (HCHO) removal.

jesc.ac.cn

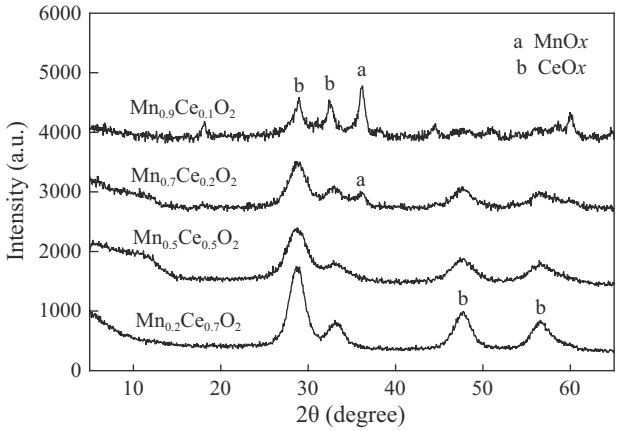

Fig. 2 – XRD patterns of $Mn_xCe_{1-x}O_2$ mixed oxides.

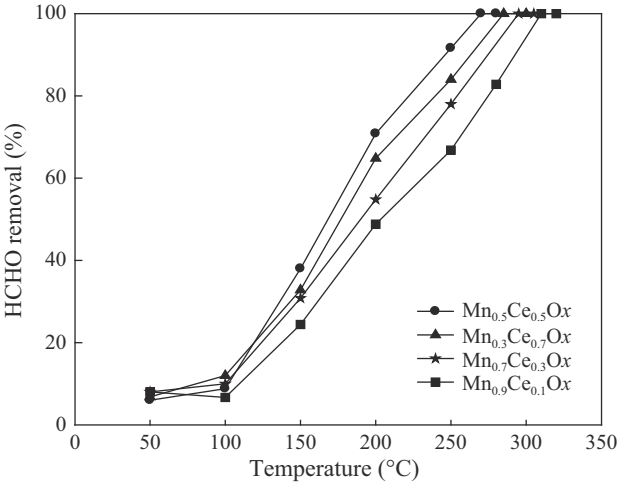

Fig. 3 – Temperature dependence of the removal efficiencies of HCHO over various catalysts. Conditions: HCHO = 33 ppm, O_2 = 21%, air as carrier gas, GHSV = 10,000 hr^{-1}.

activity and reduces T_{100}. A previous study indicated that it has good solid solution as the fraction of incorporated manganese is fixed at 0.5 (Tang et al., 2006b), which result is consistent with XRD analysis and identification.

2.3. HCHO removal by TCO with various supports

Cu is loaded onto various supports including $Mn_{0.5}Ce_{0.5}O_2$, TiO_2, γ-Al_2O_3 and CeO_2 for effective HCHO removal. Fig. 4 shows that the catalytic activity of supported Cu catalysts of HCHO oxidation depended significantly on the support material. The mixed oxide $CuO_x/Mn_{0.5}Ce_{0.5}O_2$ exhibited the highest activity in HCHO oxidation. The T_{100} of HCHO oxidation over 5 wt.% $CuO_x/Mn_{0.5}Ce_{0.5}O_2$ (230°C) is lower than that of $Mn_{0.5}Ce_{0.5}O_2$ (T100 = 270°C) by 40°C.

Furthermore, various supports (CeO_2, TiO_2 and γ-Al_2O_3) are compared. As indicated in Fig. 4, T_{100} of 270°C can be achieved with 5 wt.% CuO_x/CeO_2, in addition, the support TiO_2 performs worst with a T_{100} of 430°C, followed by γ-Al_2O_3 with a T_{100} of 340°C. The activities of the copper that was loaded onto CeO_2 and $Mn_{0.5}Ce_{0.5}O_2$ markedly exceeded TiO_2 and γ-Al_2O_3. The high activity was attributed to the redox interaction between CuO_x and $Mn_{0.5}Ce_{0.5}O_2$. Obviously, support is one of the important parameters that affect catalytic activity, and an increase in the redox property of the support enhances catalytic activity. MnO_x is favorable because it is easily reduced. Cerium oxide is well known for its better oxygen releasing oxygen storage capacity than other fluorite-type oxides (Imamura et al., 1996). Therefore, it is more effective in the deep oxidation of HCHO. This study exploits the advantages of the two metals manganese and cerium by using $Mn_xCe_{1-x}O_2$ mixed oxides. The catalytic activity test (Fig. 4) indicates that copper loaded on $Mn_{0.5}Ce_{0.5}O_2$ performs best for HCHO oxidation, and the T_{100} for the complete oxidation of HCHO is lower than that of copper supported on γ-Al_2O_3, TiO_2 or CeO_2. The supports in order of the activity of 5 wt.% copper on each are $Mn_{0.5}Ce_{0.5}O_2$ > CeO_2 > γ-Al_2O_3 > TiO_2. Table 1 indicates that catalyst activities are not closely correlated with the specific surface area. Apparently, the redox property of catalyst is more important in the oxidation of HCHO. The interaction between copper and $Mn_xCe_{1-x}O_2$ support positively influences both the physicochemical property and the catalytic performance of the 5 wt.% $CuO_x/Mn_{0.5}Ce_{0.5}O_2$ catalysts in the oxidation of HCHO at moderate temperature. A

Table 1 – Characterization of the catalysts.

Catalyst	EDS (wt.%)						BET (m^2/g)
	Cu	Mn	Al	Ti	Ce	O	
5 wt.% CuO_x/γ-Al_2O_3	7.12	–	55.4	–	–	37.4	111.7
5 wt.% CuO_x/TiO_2	5.06	–	–	50.1	–	44.8	53.7
5 wt.% CuO_x/CeO_2	5.31	–	–	–	51.5	43.1	90.1
5 wt.% $CuO_x/Mn_{0.5}Ce_{0.5}O_2$	6.56	37.5	–	–	43.5	12.4	39.2
$Mn_{0.5}Ce_{0.5}O_2$	–	41.2	–	–	48.3	10.5	39.3
γ-Al_2O_3	–	–	–	–	–	–	123.5
TiO_2	–	–	–	–	–	–	61.3
CeO_2	–	–	–	–	–	–	103.6

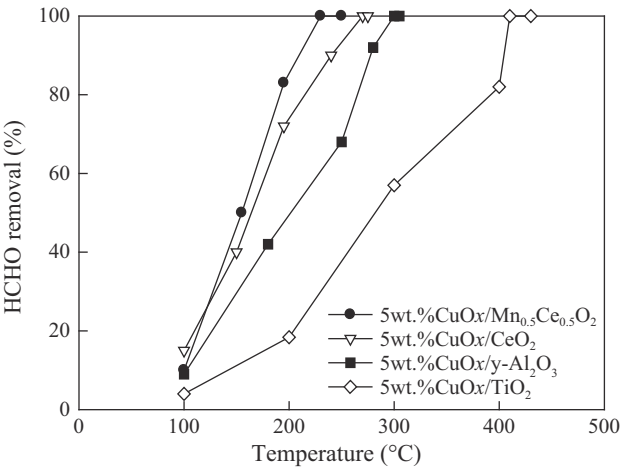

Fig. 4 – Temperature dependence of the HCHO removal efficiencies over copper catalysts on different supports. Condition: HCHO = 33 ppm, air as carrier gas, GHSV = 10,000 hr^{-1}.

jesc.ac.cn

strong metal–support interaction (SMSI) improves the release of oxygen from the support (Gil et al., 1994), improving the catalytic activity in HCHO oxidation. The crystalline phase of the solid solution has an ordered crystalline arrangement, which promotes the activity of the catalyst for HCHO oxidation.

The kinetics of the catalytic oxidation of HCHO were studied using the Mars–Van Krevelen Model. Table 2 presents the activation energies for HCHO removal obtained using three catalysts. The rate constant (k) is first determined by assuming the first-order reaction. Thereafter, values of k at different temperatures are obtained, and a straight line of ln$k$ *versus* 1/T is plotted to calculate the activation energy (E_a). The results indicate that the activation energy over 5 wt.% CuO_x/$Mn_{0.5}Ce_{0.5}O_2$ is 37.8 kJ/mol. Previous investigations indicate that the activation energies for the catalytic oxidations of HCHO over 7.1 wt.% Au/Fe–O and MnO_2 nano-rods are 26.6 and 79.8 kJ/mol, respectively (Li et al., 2008; Zhou et al., 2011).

The activation energies obtained using the supported noble metal catalysts are much lower than those obtained using transition metal catalysts, including ceria and manganese. Fig. 5 reveals that 5 wt.% CuO_x/$Mn_{0.5}Ce_{0.5}O_2$ mixed oxides were highly active in the oxidation of HCHO at moderate temperature, which had a much lower activation energy if compared with MnO_2 (Zhou et al., 2011). These results indicate that the use of noble metals rather than transition metals greatly reduces the activation energy.

2.4. Activities of various catalysts for ozone decomposition

The efficiency of ozone decomposition using a catalyst depended strongly on the conductivity of the metal of the oxide, Oyama (2000) suggested that p-type oxides such as MnO_x are more active than n-type oxides in ozone decomposition (Oyama, 2000).

Fig. 6 plots the time courses of ozone decomposition using various metal oxide catalysts including $Mn_{0.5}Ce_{0.5}O_2$, 5 wt.% CuO_x/$Mn_{0.5}Ce_{0.5}O_2$, Mn_2O_3, CeO_2 and TiO_2. All of the metal oxides that were tested in this investigation catalytically decompose ozone. The efficiency of ozone decomposition does not change significantly with time using any catalyst. The order of catalyst performance in ozone decomposition is $Mn_{0.5}Ce_{0.5}O_2$ (99.2%) > 5 wt.% CuO_x/$Mn_{0.5}Ce_{0.5}O_2$ (97.3%) > Mn_2O_3 (92.1%) > CeO_2(15.1%) > TiO_2 (9.81%). Of these oxides, Mn_2O_3, CeO_2 and CuO_2 are p-type oxides. These p-type oxides, except for CeO_2, have high activities for ozone decomposition. On the other hand, the n-type oxides such as TiO_2 have low activities for ozone decomposition. Among these catalysts, $Mn_{0.5}Ce_{0.5}O_2$ has the highest activity, reflecting the fact that mixed oxides exhibit improved catalytic activity. Apparently, the catalytic activity of the metal element is an important parameter in the decomposition of ozone.

Table 2 – Activation energies for the oxidation of formaldehyde (HCHO) under various conditions.

Catalyst	Activation energy (kJ/mol)	Temperature range (°C)	Reference
5 wt.% CuO_x/$Mn_{0.5}Ce_{0.5}O_2$	37.8	100–200	This study
7.1 wt.% Au/Fe–O	26.6	20–100	Li et al. (2008)
MnO_2 ramsdellite nanorods	79.8	80–120	Zhou et al. (2011)

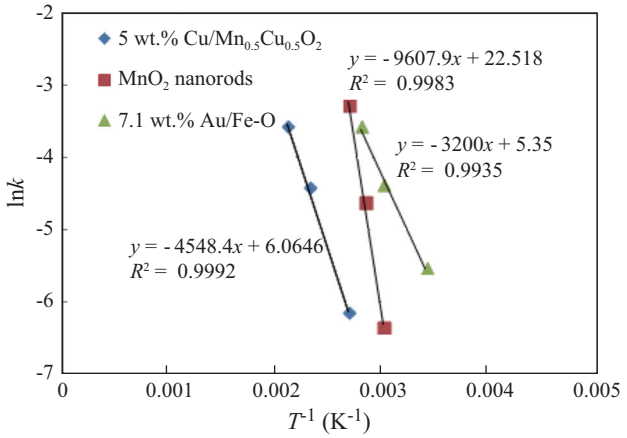

Fig. 5 – Arrhenius dependency of rate constant and temperature for HCHO oxidation at a fixed HCHO concentration.

2.5. Removal of HCHO by OZCO

The performances of various catalysts in the removal of HCHO with OZCO were investigated at room temperature (Fig. 7). The inlet HCHO concentration was controlled at 61 ppm while ozone concentration was fixed at 203 ppm. The efficiency of HCHO removal using CeO_2 catalyst was only 13.4%; that of Mn-oxide catalysts was much higher. $Mn_{0.5}Ce_{0.5}O_2$ catalyst provides an HCHO removal efficiency of up to 83.1%, and HCHO removal efficiency can also achieve 82% and 78% as 5 wt.% CuO_x/$Mn_{0.5}Ce_{0.5}O_2$ and Mn_2O_3 are applied, respectively. Overall, HCHO removal efficiency increases with increasing ozone decomposition efficiency. Among these, the manganese-oxide series of catalysts have better catalytic performance than other metal catalysts. In particular, partial substitution of Ce^{4+} by Mn^{4+} in the CeO_2 lattice leads to the formation of a solid solution with the improvement of ozone decomposition and

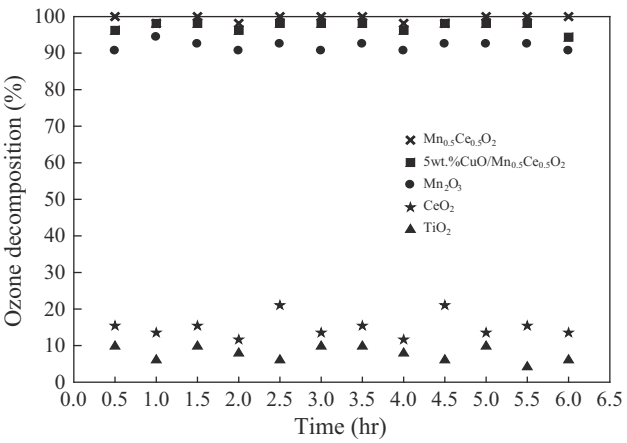

Fig. 6 – Time courses for ozone decomposition over metal oxide supported. Conditions: Ozone = 1000 ppm, air as carrier gas, GHSV = 10,000 hr^{-1}, T = 25°C.

jesc.ac.cn

HCHO removal capacity (Luo et al., 1999). However, activity of 5 wt.% $CuO_x/Mn_{0.5}Ce_{0.5}O_2$ was slightly lower for HCHO removal if compared with $Mn_{0.5}Ce_{0.5}O_2$. Presumably, the element of copper affects area of contact of $Mn_{0.5}Ce_{0.5}O_2$ and ozone, because copper was loaded on $Mn_{0.5}Ce_{0.5}O_2$ by impregnation method, hence, it may reduce ozone decomposition efficiency. A previous study indicates that efficiency of ozone decomposition was decreased with increasing content of Cu, in addition, its reaction temperature must be increased to least at 60°C for effective ozone decomposition, implying that activity of Cu is lower for ozone decomposition if compared with Mn-based catalysts (Spasova et al., 2007). Accordingly, $Mn_{0.5}Ce_{0.5}O_2$ is used as the catalyst removal for HCHO in the following experiments.

2.6. Effect of O_3/HCHO ratio on HCHO removal

In the catalytic oxidation process using ozone, the dose of ozone is an important parameter that affects HCHO removal efficiency. Each O_3 molecule is dissociated into one atomic oxygen species and one O_2 molecule on the catalyst according to Eq. (4). Owing to the strong capability of intermediate species to catalyze oxidation, atomic oxygen and active peroxide species are formed.

$$O_3 + * \rightarrow O_2 + O^* \quad (4)$$

where, * denotes an active site on the surface of the catalyst. According to Eq. (5), the stoichiometric molar ratio of O_3/HCHO = 2 for complete oxidation of HCHO. To improve the removal efficiency, the amount of ozone is added two to five times that required by the stoichiometric molar ratio. As presented in Fig. 8, as O_3/HCHO ratio was increased from 3 to 8, the removal HCHO efficiency increased from 83.3% to 100% while inlet HCHO concentration was controlled at 61 ppm. A similar trend was reported by Zhao et al. (2012a). However, the ozone decomposition efficiency was fairly constant, being 97.3% for a range of ozone concentrations.

$$HCHO_{(g)} + 2O_3 \rightarrow CO_2 + H_2O_{(g)} + 2O_{2(g)} \quad (5)$$

2.7. Effect of O_3 concentration on HCHO removal efficiency and mineralization

Under operating conditions of a gas hour space velocity of 10,000 hr^{-1}, O_3/HCHO = 3 and a room temperature, CO_2 was the only carbon-containing product detected in the effluent gas stream. Fig. 8 plots HCHO removal and CO_2 formation at various ratios of O_3/HCHO by using $Mn_{0.5}Ce_{0.5}O_2$ catalyst. The results indicate that the mineralization efficiency was 68% as O_3/HCHO ratio was controlled at 3. As O_3/HCHO ratio was increased to 8, 86.1% of mineralization efficiency was achieved. The removal efficiency of HCHO and the mineralization efficiency increased with ozone concentration. Therefore, as the O_3 concentration increased, the amount of atomic oxygen that was formed on the surface of the catalyst increased, causing deeper oxidation. In addition, a previous study indicates that mineralization efficiency can be possibly increased to 100% by introducing small amount of $H_2O_{(g)}$, since hydroxyl radicals are the predominant oxidative species in the presence of ozone and water vapor (Zhao et al., 2012b). Furthermore, HCHO can be oxidized to CO_2 by the chemisorbed hydroxyl radicals generated from the ozone decomposition in the presence of $H_2O_{(g)}$ on the catalysts surface. However, the effect of $H_2O_{(g)}$ on HCHO removal was not investigated in this study.

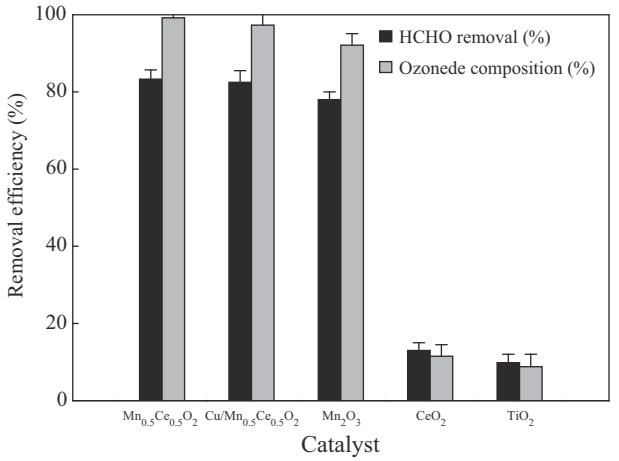

Fig. 7 – HCHO removal efficiency achieved with different catalysts. Conditions: HCHO = 61 ppm and air as carrier gas, O_3 = 203 ppm, GHSV = 10,000 hr^{-1}, T = 25°C.

2.8. Durability test

The durability of catalysts is very important in determining their practical usefulness. Fig. 9 indicates that the removal efficiency of HCHO was about 7.23% in the initial period of the reaction (Stage I, without ozone), increasing to 81.2% after 9 hr (Stage II, with ozone). As presented in Fig. 9, no significant deactivation was observed following operation for 80 hr, revealing that the $Mn_{0.5}Ce_{0.5}O_2$ catalyst of HCHO removal was highly durable.

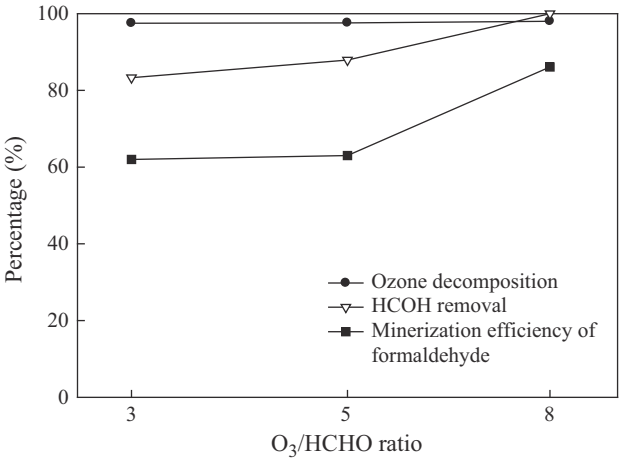

Fig. 8 – Effect of O_3/HCHO ratio on HCHO removal and mineralization efficiency. Conditions: HCHO = 61 ppm and air as carrier gas, O_3 = 203–506 ppm, GHSV = 10,000 hr^{-1}, T = 25°C.

jesc.ac.cn

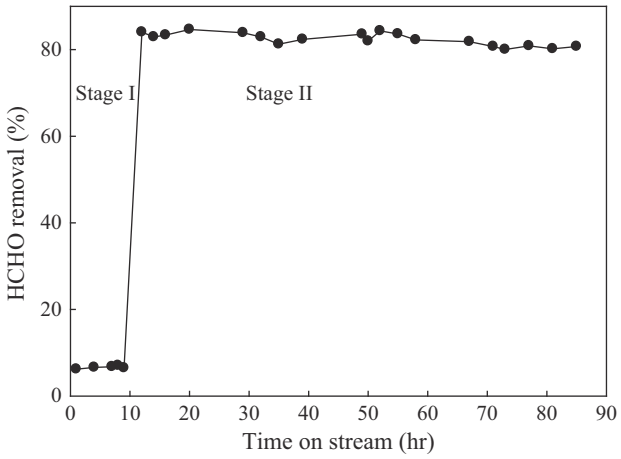

Fig. 9 – Durability test on the $Mn_{0.5}Ce_{0.5}O_2$ catalyst for HCHO oxidation. Conditions: HCHO = 61 ppm, GHSV = 10,000 hr^{-1}, T = 25°C; Stage I: air as carrier gas; Stage II: O_3 = 203 ppm.

3. Conclusions

In this work, incorporation of manganese into CeO_2 to form $Mn_xCe_{1-x}O_2$ solid solution increased the mobility of the lattice oxygen and markedly improved the performance of the catalyst in the oxidation of HCHO. The HCHO removal efficiency was 83.3% at 25°C and O_3/HCHO = 3; the same removal efficiency was obtained when TCO was operated at 185°C. A strong correlation was observed between the removal efficiencies of HCHO and ozone. These demonstrate that the reaction temperature, species of catalyst and ozone concentration all had to be optimized to ensure the complete oxidation of HCHO to CO_2. This work reports on the catalytic oxidation of HCHO with ozone over supported $Mn_{0.5}Ce_{0.5}O_2$ catalysts at room temperature. Overall, this OZCO process uses eco-friendly, cost-effective manganese oxide catalysts to remove HCHO. Adding appropriate amount of ozone to the OZCO system results in the effective removal of HCHO at room temperature. The method can be utilized directly to reduce industrial emissions and control the quality of indoor air.

REFERENCES

Álvarez-Galván, M.C., Pawelec, B., de la Pena O'Shea, V.A., Fierro, J.L.G., Arias, P.L., 2004. Formaldehyde/methanol combustion on alumina-supported manganese–palladium oxide catalyst. Appl. Catal. B 51 (2), 83–91.

An, N., Yu, Q., Liu, G., Li, S., Jia, M., Zhang, W., 2011. Complete oxidation of formaldehyde at ambient temperature over supported Pt/Fe_2O_3 catalysts prepared by colloid-deposition method. J. Hazard. Mater. 186 (2–3), 1392–1397.

Chen, B.B., Shi, C., Crocker, M., Wang, Y., Zhu, A.M., 2013. Catalytic removal of formaldehyde at room temperature over supported gold catalysts. Appl. Catal. B 132–133, 245–255.

Daisey, J.M., Angell, W.J., Apte, M.G., 2003. Indoor air quality, ventilation and health symptoms in schools: an analysis of existing information. Indoor Air 13 (1), 53–64.

Dhandapani, B., Oyama, S.T., 1997. Gas phase ozone decomposition catalysts. Appl. Catal. B 11 (2), 129–166.

Einaga, H., Futamura, S., 2004a. Comparative study on the catalytic activities of alumina-supported metal oxides for oxidation of benzene and cyclohexane with ozone. React. Kinet. Catal. Lett. 81 (1), 121–128.

Einaga, H., Futamura, S., 2004b. Catalytic oxidation of benzene with ozone over alumina-supported manganese oxides. J. Catal. 227 (2), 304–312.

Einaga, H., Futamura, S., 2005. Oxidation behavior of cyclohexane on alumina-supported manganese oxides with ozone. Appl. Catal. B 60 (1–2), 49–55.

Gervasini, A., Vezzoli, G.C., Ragaini, V., 1996. VOC removal by synergic effect of combustion catalyst and ozone. Catal. Today 29 (1–4), 449–455.

Gil, A., Díaz, A., Gandía, L.M., Montes, M., 1994. Influence of the preparation method and the nature of the support on the stability of nickel catalysts. Appl. Catal. A 109 (2), 167–179.

Góra-Marek, K., Datka, J., 2008. The transformation of formaldehyde on CoZSM-5 zeolites. Catal. Today 137 (2–4), 466–470.

Gracia, R., Cortes, S., Sarasa, J., Ormad, P., Ovelleiro, J.L., 2000. Catalytic ozonation with supported titanium dioxide. The stability of catalyst in water. Ozone Sci. Eng. 22 (2), 185–193.

Imamura, S., Uchihori, D., Utani, K., Ito, T., 1994. Oxidative decomposition of formaldehyde on silver–cerium composite oxide catalyst. Catal. Lett. 24 (3–4), 377–384.

Imamura, S., Shono, M., Okamoto, N., Hamada, A., Ishida, S., 1996. Effect of cerium on the mobility of oxygen on manganese oxides. Appl. Catal. A 142 (2), 279–288.

Konova, P., Stoyanova, M., Naydenov, A., Christoskova, St., Mehandjiev, D., 2006. Catalytic oxidation of VOCs and CO by ozone over alumina supported cobalt oxide. Appl. Catal. A 298 (10), 109–114.

Li, C.Y., Shen, Y.N., Jia, M.L., Sheng, S.S., Adebaj, M.O., Zhu, H.Y., 2008. Catalytic combustion of formaldehyde on gold/iron-oxide catalysts. Catal. Commun. 9 (3), 355–361.

Luo, M.F., Zheng, X.M., Zhong, Y.J., 1999. CO oxidation activity and TPR characterization of CeO_2-supported manganese oxide catalysts. Indian J. Chem. Sect. A 38A (7), 703–707.

Ma, C., Wang, D., Xue, W., Dou, B., Wang, H., Hao, Z., 2011. Investigation of formaldehyde oxidation over Co_3O_4–CeO_2 and Au/Co_3O_4–CeO_2 catalysts at room temperature: effective removal and determination of reaction mechanism. Environ. Sci. Technol. 45 (8), 3628–3634.

Oyama, S.T., 2000. Chemical and catalytic properties of ozone. Catal. Rev. Sci. Eng. 42 (3), 279–322.

Sekine, Y., 2002. Oxidative decomposition of formaldehyde by metal oxides at room temperature. Atmos. Environ. 36 (35), 5543–5547.

Shaughnessy, R.J., Levetin, E., Blocker, J., Sublette, K.L., 1994. Effectiveness of portable indoor air cleaners: sensory testing results. Indoor Air 4 (3), 179–188.

Shi, S., Wang, Y., Zhu, A.M., Chen, B.B., Au, C., 2012a. $Mn_xCo_{3-x}O_4$ solid solution as high-efficient catalysts for low-temperature oxidation of formaldehyde. Catal. Commun. 28, 18–22.

Shi, S., Chen, B.B., Li, X.S., Crocker, M., Wang, Y., Zhu, A.M., 2012b. Catalytic formaldehyde removal by "storage-oxidation" cycling process over supported silver catalysts. Chem. Eng. J. 200–202, 729–737.

Silva, A.M.T., Marques, R.R.N., Quinta-Ferreira, R.M., 2004. Catalysts based in cerium oxide for wet oxidation of acrylic acid in the prevention of environmental risks. Appl. Catal. B 47 (4), 269–279.

Spasova, I., Nikolov, P., Mehandjiev, D., 2007. Ozone decomposition over alumina-supported copper, manganese and copper–manganese catalysts. Ozone Sci. Eng. 29 (1), 41–45.

Stoyanova, M., Konova, P., Nikolov, P., Naydenov, A., Christoskova, St, Mehandjiev, D., 2006. Alumina-supported nickel oxide for ozone decomposition and catalytic ozonation of CO and VOCs. Chem. Eng. J. 122 (1–2), 41–46.

jesc.ac.cn

Tang, X., Chen, J., Li, Y., Li, Y., Xu, Y., Xu, W., 2006a. Complete oxidation of formaldehyde over Ag/MnO_x–CeO_2 catalysts. Chem. Eng. J. 118 (1–2), 119–125.

Tang, X., Li, Y., Huang, X., Xu, Y., Zhu, H., Wang, J., et al., 2006b. MnO_x–CeO_2 mixed oxide catalysts for complete oxidation of formaldehyde: effect of preparation method and calcination temperature. Appl. Catal. B 62 (3–4), 265–273.

Wang, H.C., Liang, H.S., Chang, M.B., 2011. Chlorobenzene oxidation using ozone over iron oxide and manganese oxide catalysts. J. Hazard. Mater. 186 (2–3), 1781–1787.

Zhang, C., He, H., Tanaka, K.I., 2006. Catalytic performance and mechanism of a Pt/TiO_2 catalyst for the oxidation of formaldehyde at room temperature. Appl. Catal. B 65 (1–2), 37–43.

Zhang, J., Jin, Y., Li, C., Shen, Y., Han, L., Hu, Z., et al., 2009. Creation of three-dimensionally ordered macroporous Au/CeO_2 catalysts with controlled pore sizes and their enhanced catalytic performance for formaldehyde oxidation. Appl. Catal. B 91 (1–2), 11–20.

Zhao, D.Z., Ding, T., Li, X., Liu, J., Shi, C., Zhu, A.M., 2012a. Ozone catalytic oxidation of HCHO in air over MnO_x at room temperature. Chin. J. Catal. 33 (2–3), 396–401.

Zhao, D.Z., Shi, C., Li, X.S., Zhu, A.M., Jang, B.W.L., 2012b. Enhanced effect of water vapor on complete oxidation of formaldehyde in air with ozone over MnO_x catalysts at room temperature. J. Hazard. Mater. 239–240, 362–369.

Zhou, L., Zhang, J., He, J., Hu, Y., Tina, H., 2011. Control over the morphology and structure of manganese oxide by tuning reaction conditions and catalytic performance for formaldehyde oxidation. Mater. Res. Bull. 46 (10), 1714–1722.

jesc.ac.cn

Editorial Board of Journal of Environmental Sciences

Editor-in-Chief

Hongxiao Tang Research Center for Eco-Environmental Sciences, Chinese Academy of Sciences, China

Associate Editors-in-Chief

Jiuhui Qu Research Center for Eco-Environmental Sciences, Chinese Academy of Sciences, China
Shu Tao Peking University, China
Nigel Bell Imperial College London, United Kingdom
Po-Keung Wong The Chinese University of Hong Kong, Hong Kong, China

Editorial Board

Aquatic environment

Baoyu Gao
Shandong University, China
Maohong Fan
University of Wyoming, USA
Chihpin Huang
National Chiao Tung University
Taiwan, China
Ng Wun Jern
Nanyang Environment &
Water Research Institute, Singapore
Clark C. K. Liu
University of Hawaii at Manoa, USA
Hokyong Shon
University of Technology, Sydney, Australia
Zijian Wang
Research Center for Eco-Environmental Sciences,
Chinese Academy of Sciences, China
Zhiwu Wang
The Ohio State University, USA
Yuxiang Wang
Queen's University, Canada
Min Yang
Research Center for Eco-Environmental Sciences,
Chinese Academy of Sciences, China
Zhifeng Yang
Beijing Normal University, China
Han-Qing Yu
University of Science & Technology of China

Terrestrial environment

Christopher Anderson
Massey University, New Zealand
Zucong Cai
Nanjing Normal University, China
Xinbin Feng
Institute of Geochemistry,
Chinese Academy of Sciences, China
Hongqing Hu
Huazhong Agricultural University, China
Kin-Che Lam
The Chinese University of Hong Kong
Hong Kong, China
Erwin Klumpp
Research Centre Juelich, Agrosphere Institute
Germany
Peijun Li
Institute of Applied Ecology,
Chinese Academy of Sciences, China
Michael Schloter
German Research Center for Environmental Health
Germany
Xuejun Wang
Peking University, China
Lizhong Zhu
Zhejiang University, China

Atmospheric environment

Jianmin Chen
Fudan University, China
Abdelwahid Mellouki
Centre National de la Recherche Scientifique
France
Yujing Mu
Research Center for Eco-Environmental Sciences,
Chinese Academy of Sciences, China
Min Shao
Peking University, China
James Jay Schauer
University of Wisconsin-Madison, USA
Yuesi Wang
Institute of Atmospheric Physics,
Chinese Academy of Sciences, China
Xin Yang
University of Cambridge, UK

Environmental biology

Yong Cai
Florida International University, USA
Henner Hollert
RWTH Aachen University, Germany
Jae-Seong Lee
Sungkyunkwan University, South Korea
Christopher Rensing
University of Copenhagen, Denmark
Bojan Sedmak
National Institute of Biology, Slovenia
Lirong Song
Institute of Hydrobiology,
Chinese Academy of Sciences, China
Chunxia Wang
National Natural Science Foundation of China
Gehong Wei
Northwest A & F University, China
Daqiang Yin
Tongji University, China
Zhongtang Yu
The Ohio State University, USA

Environmental toxicology and health

Jingwen Chen
Dalian University of Technology, China
Jianying Hu
Peking University, China
Guibin Jiang
Research Center for Eco-Environmental Sciences,
Chinese Academy of Sciences, China
Sijin Liu
Research Center for Eco-Environmental Sciences,
Chinese Academy of Sciences, China
Tsuyoshi Nakanishi
Gifu Pharmaceutical University, Japan
Willie Peijnenburg
University of Leiden, The Netherlands
Bingsheng Zhou
Institute of Hydrobiology,
Chinese Academy of Sciences, China

Environmental catalysis and materials

Hong He
Research Center for Eco-Environmental Sciences,
Chinese Academy of Sciences, China
Junhua Li
Tsinghua University, China
Wenfeng Shangguan
Shanghai Jiao Tong University, China
Yasutake Teraoka
Kyushu University, Japan
Ralph T. Yang
University of Michigan, USA

Environmental analysis and method

Zongwei Cai
Hong Kong Baptist University,
Hong Kong, China
Jiping Chen
Dalian Institute of Chemical Physics,
Chinese Academy of Sciences, China
Minghui Zheng
Research Center for Eco-Environmental Sciences,
Chinese Academy of Sciences, China

Municipal solid waste and green chemistry

Pinjing He
Tongji University, China

Environmental ecology

Rusong Wang
Research Center for Eco-Environmental Sciences,
Chinese Academy of Sciences, China

Editorial office staff

Managing editor Qingcai Feng
Editors Zixuan Wang Suqin Liu Zhengang Mao
English editor Catherine Rice (USA)

Copyright© Research Center for Eco-Environmental Sciences, Chinese Academy of Sciences. Published by Elsevier B.V. and Science Press. All rights reserved.

JOURNAL OF ENVIRONMENTAL SCIENCES

环境科学学报(英文版)

(http://www.jesc.ac.cn)

Aims and scope

Journal of Environmental Sciences is an international academic journal supervised by Research Center for Eco-Environmental Sciences, Chinese Academy of Sciences. The journal publishes original, peer-reviewed innovative research and valuable findings in environmental sciences. The types of articles published are research article, critical review, rapid communications, and special issues.

The scope of the journal embraces the treatment processes for natural groundwater, municipal, agricultural and industrial water and wastewaters; physical and chemical methods for limitation of pollutants emission into the atmospheric environment; chemical and biological and phytoremediation of contaminated soil; fate and transport of pollutants in environments; toxicological effects of terrorist chemical release on the natural environment and human health; development of environmental catalysts and materials.

For subscription to electronic edition

Elsevier is responsible for subscription of the journal. Please subscribe to the journal via http://www.elsevier.com/locate/jes.

For subscription to print edition

China: Please contact the customer service, Science Press, 16 Donghuangchenggen North Street, Beijing 100717, China. Tel: +86-10-64017032; E-mail: journal@mail.sciencep.com, or the local post office throughout China (domestic postcode: 2-580).

Outside China: Please order the journal from the Elsevier Customer Service Department at the Regional Sales Office nearest you.

Submission declaration

Submission of an article implies that the work described has not been published previously (except in the form of an abstract or as part of a published lecture or academic thesis), that it is not under consideration for publication elsewhere. The submission should be approved by all authors and tacitly or explicitly by the responsible authorities where the work was carried out. If the manuscript accepted, it will not be published elsewhere in the same form, in English or in any other language, including electronically without the written consent of the copyright-holder.

Submission declaration

Submission of the work described has not been published previously (except in the form of an abstract or as part of a published lecture or academic thesis), that it is not under consideration for publication elsewhere. The publication should be approved by all authors and tacitly or explicitly by the responsible authorities where the work was carried out. If the manuscript accepted, it will not be published elsewhere in the same form, in English or in any other language, including electronically without the written consent of the copyright-holder.

Editorial

Authors should submit manuscript online at http://www.jesc.ac.cn. In case of queries, please contact editorial office, Tel: +86-10-62920553, E-mail: jesc@263.net, jesc@rcees.ac.cn. Instruction to authors is available at http://www.jesc.ac.cn.

Journal of Environmental Sciences (Established in 1989)

Vol. 26 No. 12 2014

Supervised by	Chinese Academy of Sciences	**Published by**	Science Press, Beijing, China
Sponsored by	Research Center for Eco-Environmental		Elsevier Limited, The Netherlands
	Sciences, Chinese Academy of Sciences	**Distributed by**	
Edited by	Editorial Office of Journal of	Domestic	Science Press, 16 Donghuangchenggen
	Environmental Sciences		North Street, Beijing 100717, China
	P. O. Box 2871, Beijing 100085, China		Local Post Offices through China
	Tel: 86-10-62920553; http://www.jesc.ac.cn	Foreign	Elsevier Limited
	E-mail: jesc@263.net, jesc@rcees.ac.cn		http://www.elsevier.com/locate/jes
Editor-in-chief	Hongxiao Tang	**Printed by**	Beijing Beilin Printing House, 100083, China

CN 11-2629/X **Domestic postcode: 2-580** **Domestic price per issue RMB ¥ 110.00**

ISSN 1001-0742